Simultaneous State Measurement of Coupled Josephson Phase Qubits

R. McDermott,[1] R.W. Simmonds,[2] M. Steffen,[1] K.B. Cooper,[1]
K. Cicak,[2] K.D. Osborn,[2] S. Oh,[2] D.P. Pappas,[2] and John M. Martinis[1*]

[1]Department of Physics, University of California,
Santa Barbara, CA 93106, USA
[2]National Institute of Standards and Technology,
325 Broadway, Boulder, CO 80305, USA
[*]To whom correspondence should be addressed; E-mail: martinis@physics.ucsb.edu.

One of the many challenges of building a scalable quantum computer is single-shot measurement of all the quantum bits (qubits). We have used simultaneous single-shot measurement of coupled Josephson phase qubits to directly probe interaction of the qubits in the time domain. The concept of measurement crosstalk is introduced, and we show that its effects are minimized by careful adjustment of the timing of the measurements. We observe the antiphase oscillation of the two-qubit $|01\rangle$ and $|10\rangle$ states, consistent with quantum mechanical entanglement of these states, thereby opening the possibility for full characterization of multi-qubit gates and elementary quantum algorithms.

Considerable progress has been made toward the implementation of a quantum computer (*1*) based on superconductors. Coherent single qubit operations have been shown in Josephson flux (*2*) and phase (*3*) qubits, and the time domain interaction of coupled qubits (*4*) and a controlled-NOT logic gate (*5*) have been demonstrated in the Josephson charge qubit (*6, 7*).

Previous studies of coupled superconducting qubits have relied on separate measurements of the individual qubits (bitwise readout). Such an approach does not yield complete information about the system and fails, for example, to directly establish correlations between the qubits in the case of an entangled state. In order to test quantum algorithms efficiently, or to perform quantum state tomography and thereby definitively prove entanglement, it is necessary to measure all the qubits simultaneously (wordwise readout) and with high fidelity. For multi-qubit circuits with fixed coupling - a common architecture for superconducting qubits - realization of this goal is complicated by measurement crosstalk: measurement of the state of one qubit may perturb the state of other qubits, destroying information about quantum correlations. While continued progress toward the realization of quantum gates in superconducting circuits will depend on a thorough understanding of measurement crosstalk, this issue has received little attention to date.

We describe simultaneous single-shot state measurements to probe the interaction of coupled Josephson phase qubits in the time domain. The observed antiphase oscillation of the occupation probabilities of the two-qubit basis states $|01\rangle$ and $|10\rangle$ is consistent with quantum mechanical entanglement of these states. Moreover, the free evolution between the $|01\rangle$ and $|10\rangle$ states contains the essential ingredient of the two-qubit imaginary-SWAP (*i*-SWAP) operation which, taken together with single-qubit rotations, forms a universal set of quantum gates (*8*). Our results depend crucially on a scheme for fast ($\sim$ ns) state measurement and accurate adjustment of the timing of the measurements of the two qubits in order to circumvent measurement crosstalk in the circuit. The characteristic decay time for the two-qubit oscillations is consistent with the longitudinal relaxation time of the single-qubit circuit, suggesting that little additional dissipation is introduced by coupling the qubits. This bodes well for future tests of multi-qubit gates and for more rigorous demonstrations of quantum correlations in multi-qubit circuits.

The Josephson qubit can be thought of as a manufactured electrical "atom", having discrete energy levels which exist in a potential energy landscape determined by the circuit design parameters and bias (see Figs. 1A,B for details). We have previously demonstrated high-resolution spectroscopy and coherent oscillations in the time domain in a single-qubit circuit (*9*, *10*). To implement a coupled qubit circuit, we connected two flux-biased phase qubits via a thin-film capacitor (*11*) (Fig. 1C). We label the qubits A and B. The interaction Hamiltonian can be written

$$H_{int} = \frac{S}{2}(|01\rangle\langle 10| + |10\rangle\langle 01|), \tag{1}$$

where $|01\rangle \equiv |0_A 1_B\rangle$. In terms of the circuit parameters, the coupling strength is $S \approx (C_x/C_j)\hbar\omega_{10}$, where C_x is the coupling capacitance and C_j is the junction self-capacitance. The interaction can be controlled by adjusting the flux bias of the qubits to change ω_{10}, bringing the qubits in and out of resonance. When the qubits are tuned to resonance (see inset, Fig. 2A), the eigenstates are the (entangled) symmetric and antisymmetric combinations of $|01\rangle$ and $|10\rangle$, with eigenenergies $-S/2$ and $S/2$, respectively. Far from resonance, the system behaves as two independent qubits.

Because our circuit is a manufactured quantum system, the energy levels are not known a priori; therefore it is first necessary to map out the qubit resonance frequencies versus bias using spectroscopy (*12*). In the frequency domain, the interaction is manifested as an avoided level crossing at the point where the resonant frequencies of the two qubits are matched (*13*). We biased qubit A to yield a resonant frequency $\omega_{10A}/2\pi$ of 8.65 GHz (*14*). Subsequent spectroscopy of qubit B revealed a splitting S/h = 80 MHz centered at 8.65 GHz (not shown). The measured splitting is consistent with the estimated coupling capacitance and junction self-capacitance of 6 fF and 700 fF, respectively, which are close to the design values.

We next investigated the interaction of the two qubits in the time domain. The qubits were tuned into resonance and initialized in the ground state $|00\rangle$. We then applied an 8.65 GHz

microwave π pulse to qubit A to prepare the state $|10\rangle$ (Fig. 2A inset). As this state is not an eigenstate of the two-qubit Hamiltonian, it undergoes free evolution in the subspace spanned by the vectors $|01\rangle$ and $|10\rangle$, according to the relation

$$|\Psi(t)\rangle = \frac{1}{2}(|10\rangle + |01\rangle)e^{\frac{iS}{2\hbar}t} + \frac{1}{2}(|10\rangle - |01\rangle)e^{-\frac{iS}{2\hbar}t}$$
$$= \cos\left(\frac{S}{2\hbar}t\right)|10\rangle + i\sin\left(\frac{S}{2\hbar}t\right)|01\rangle. \quad (2)$$

Therefore, measurements of the two qubits should be anticorrelated, with a $|0\rangle$ ($|1\rangle$) for qubit A yielding a measurement of $|1\rangle$ ($|0\rangle$) for qubit B. Following a variable period of free evolution t_{free}, we applied simultaneous measurement pulses to the two qubits, yielding four possible measurement outcomes. By repeated trials (100,000 events per data point), we obtained the occupation probabilities P_{00}, P_{01}, P_{10}, and P_{11}. These probabilities (points) are plotted in Fig. 2A versus t_{free}.

The occupation probabilities P_{01} and P_{10} oscillate out of phase, in agreement with the expected anticorrelation of the states of the two qubits. Moreover, the oscillation period is consistent with the 80 MHz splitting observed in the spectroscopy of the coupled qubits. The reduced amplitude of the oscillations is consistent with simulations (solid lines) which account for a 5 ns gating time for the π pulse, a measured microwave cross-coupling from qubit A to qubit B of -10 dB, a measured 70% fidelity of the qubit state measurement (*10*), and a measured energy relaxation time T_1 for the individual qubits of 25 ns.

We next repeated the above experiment for a range of qubit detunings by adjusting the flux bias of qubit B. Figures 2B,C display the occupation probabilities P_{01} and P_{10} as functions of both t_{free} and $\omega_{10B}/2\pi$. The oscillation frequency increases and visibility decreases with detuning, resulting in a characteristic "chevron" pattern for the damped oscillations, in agreement with theoretical predictions (*10*).

We emphasize that the antiphase oscillation of the occupations of the $|01\rangle$ and $|10\rangle$ states is

most clearly seen when the timing of the measurement pulses is adjusted to ensure simultaneity. As the relative delay t_{delay} of the measurement pulses is increased beyond $\sim$ 2 ns, we observe a striking change in the character of the evolution of the occupation probabilities (Fig. 3). In the case of sequential measurements of the two qubits, measurement of the $|0\rangle$ state in the first qubit has no effect on the outcome of measurement of the second qubit. On the other hand, measurement of the $|1\rangle$ state in the first qubit results in an enhancement of the probability of measuring the $|1\rangle$ state in the second qubit. We refer to this phenomenon as measurement crosstalk.

The physical mechanism for measurement crosstalk in our circuit is the following. The measurement of a $|1\rangle$ state in the first qubit implies a tunneling event to the right-hand well of the qubit potential. The resulting oscillation in the right-hand well produces a microwave voltage pulse (from the ac Josephson relation). This voltage drives a transient current $I_x(t)$ to the second qubit and induces transitions from the ground state. Because the qubits are weakly coupled ($C_x \ll C_j$), the effect of the current $I_x(t)$ can be understood by treating it as a classical drive to the second qubit. Numerical simulations indicate that the ringup of the second qubit can be separated into three segments in time (Figs. 4A,B): (I) The initial oscillation in the right-hand well of the measured qubit samples the region near the turning point at the top of the well, corresponding to frequencies below the resonance frequency of the second qubit. The resulting drive current is off resonance with the second qubit; therefore, no appreciable coupling occurs for a time $\sim 0.1T_1$. (II) As the oscillations damp and come into resonance with the second qubit, the energy transferred to the second qubit is roughly quadratic in time, and can be parametrized as $E_x/\hbar\omega_{10} \sim 10(C_x/C_j)^2[\omega_{10}(t_{delay} - 0.1T_1)]^2$. (III) Finally, as the measured qubit continues to decay and begins to sample the deepest, harmonic regions of the right-hand well, the oscillation frequency moves above the resonance frequency of the second qubit. No additional energy is added, and the energy transferred to the second qubit levels out at a value

$E_x/\hbar\omega_{10} \sim 100(C_x/C_j)^2\omega_{10}T_1$. Taking the probability for an $|0\rangle \rightarrow |1\rangle$ transition to be $P_1 \approx E_x/\hbar\omega_{10}$ for $E_x/\hbar\omega_{10} \ll 1$, we predict minimal measurement crosstalk for our circuit for $|t_{delay}| < 2$ ns. Moreover, we note that the constraint on measurement timing becomes *less* stringent for qubits with longer T_1.

The dependence of measurement crosstalk on timing of the measurements was investigated by repeating the experiment of Fig. 2 while varying t_{delay} to cover a total range of $\pm$4 ns (Fig. 4C). When $t_{delay} > 2$ ns ($t_{delay} < 2$ ns), the probability P_{11} is correlated with P_{10} (P_{01}). It is only when the relative delay of the measurements is optimally adjusted ($|t_{delay}| < 2$ ns) that P_{11} is small and the oscillations in P_{11} disappear. Separate experiments indicate that when the timing of the measurement pulses is optimized, a tunneling event in one qubit results in a false measurement of $|1\rangle$ in the second qubit with only 15% probability. This residual measurement crosstalk can be attributed to the finite duration of the measurement pulse.

Our results suggest that it is possible in principle to perform high fidelity measurements of multiple qubits, and therefore provide a promising outlook for scalable quantum information processing based on Josephson junctions.

References and Notes

1. M.A. Nielsen and I.L. Chuang, *Quantum Computation and Quantum Information* (Cambridge Univ. Press, Cambridge, 2000).

2. I. Chiorescu, Y. Nakamura, C.J.P.M. Harmans, J.E. Mooij, *Science* **299**, 1896 (2003).

3. J.M. Martinis, S. Nam, J. Aumentado, C. Urbina, *Phys. Rev. Lett.* **89**, 117901 (2002).

4. Yu.A. Pashkin *et al.*, *Nature* **421**, 823 (2003).

5. T. Yamamoto, Yu.A. Pashkin, O. Astafiev, Y. Nakamura, J.S. Tsai, *Nature* **425**, 941 (2003).

6. Y. Nakamura, Yu.A. Pashkin, J.S. Tsai, *Nature* **398**, 786 (1999).

7. D. Vion *et al.*, *Science* **296**, 886 (2002).

8. J. Kempe, K.B. Whaley, *Phys. Rev. A* **65**, 052330 (2002).

9. R.W. Simmonds, K.M. Lang, D.A. Hite, D.P. Pappas, J.M. Martinis, *Phys. Rev. Lett.* **93**, 077003 (2004).

10. K.B. Cooper *et al.*, *Phys. Rev. Lett.* **93**, 180401 (2004).

11. P.R. Johnson *et al.*, *Phys. Rev. B* **67**, 020509 (2003).

12. J.M. Martinis, M.H. Devoret, J.Clarke, *Phys. Rev. Lett* **55**, 1543 (1985).

13. A.J. Berkley *et al.*, *Science* **300**, 1548 (2003).

14. At this frequency, the spectra of both qubits were free of fine structure due to spurious junction resonances (*9*).

15. Supported in part by NSA/ARDA through ARO research grants W911NF-04-1-2004 and MOD717304. Contribution of the U. S. government, not subject to copyright.

Fig. 1. (A),(B) Potential energy landscape for the flux-biased Josephson phase qubit. During operation, the qubit is biased so that the junction phase δ is trapped in a metastable minimum of the potential $U(\delta)$ which contains several discrete energy levels. Measurement is accomplished by a fast flux pulse which adiabatically lowers the potential barrier, inducing a tunneling transition from the $|1\rangle$ state to the right-hand well of the potential, which contains around 150 states, resulting in a flux change of $\sim 1\Phi_0 \equiv h/2e$. (C) Circuit diagram of the coupled phase qubit circuit. The qubit junctions, with self-capacitance $C_j \approx$ 700 fF, are coupled via the capacitance $C_x \approx$ 6 fF; the junction critical currents are 1.7 μA, and the qubit loop inductances are 720 pH. The qubits are capacitively coupled to the microwave control lines; each qubit loop is inductively coupled to a coil that provides both the flux bias and the measurement pulse, and to a dc SQUID (not shown) which is used to read out the flux state of the qubit loop. The devices are fabricated from *Al/AlOx/Al* trilayers using conventional thin-film techniques and optical lithography.

Fig. 2. Interaction of coupled qubits in the time domain. (A) With the qubits tuned to resonance $\omega_{10A}/2\pi = \omega_{10B}/2\pi =$ 8.65 GHz, a microwave π pulse on qubit A prepares the state $|10\rangle$. This state subsequently undergoes free precession in the subspace spanned by $|10\rangle$ and $|01\rangle$ before being measured, yielding the state $|00\rangle$, $|10\rangle$, $|01\rangle$, or $|11\rangle$. Repeated measurements give probabilities $1 - P_{00}$, P_{10}, P_{01}, P_{11}, which are plotted (points) versus free precession time t_{free}. The solid lines are from numerical simulations which assume a 5 ns gating time for the π pulse and which take into account -10 dB microwave cross coupling, 70% measurement fidelity, and a single-qubit T_1 of 25 ns, all determined experimentally from separate measurements. (B),(C) Oscillations of P_{10} and P_{01} (color scale) as qubit B is detuned from the resonance of qubit A (dashed line).

Fig. 3. Measurement crosstalk in the phase qubit, determined by sequential measurement of the states of the qubits. In Fig. 3A (3B), qubit A was measured 4 ns before (after) qubit B;

the data is plotted as in Fig. 2. The figure insets represent the currents applied to each of the qubit junctions; the microwave π pulse prepares the state $|10\rangle$, while gaussian pulses (labeled M) measure the qubit states. When qubit A is measured before (after) qubit B, the oscillations in P_{11} are correlated with the oscillations in P_{10} (P_{01}). From the relative amplitude of the oscillations we conclude that measurement of $|1\rangle$ in the first qubit results in false measurement of $|1\rangle$ in the second qubit with $\sim 70\%$ probability.

Fig. 4. Description of simultaneous measurement. (A) Numerical simulation of the energy transfer to qubit B induced by a tunneling event in qubit A. The three stages of energy transfer (see text) correspond to energy decay through regions I-III in the potential diagram (B). (C) P_{11} versus free evolution time t_{free} and relative delay t_{delay} of the measurements of the two qubits.

Fig. 1

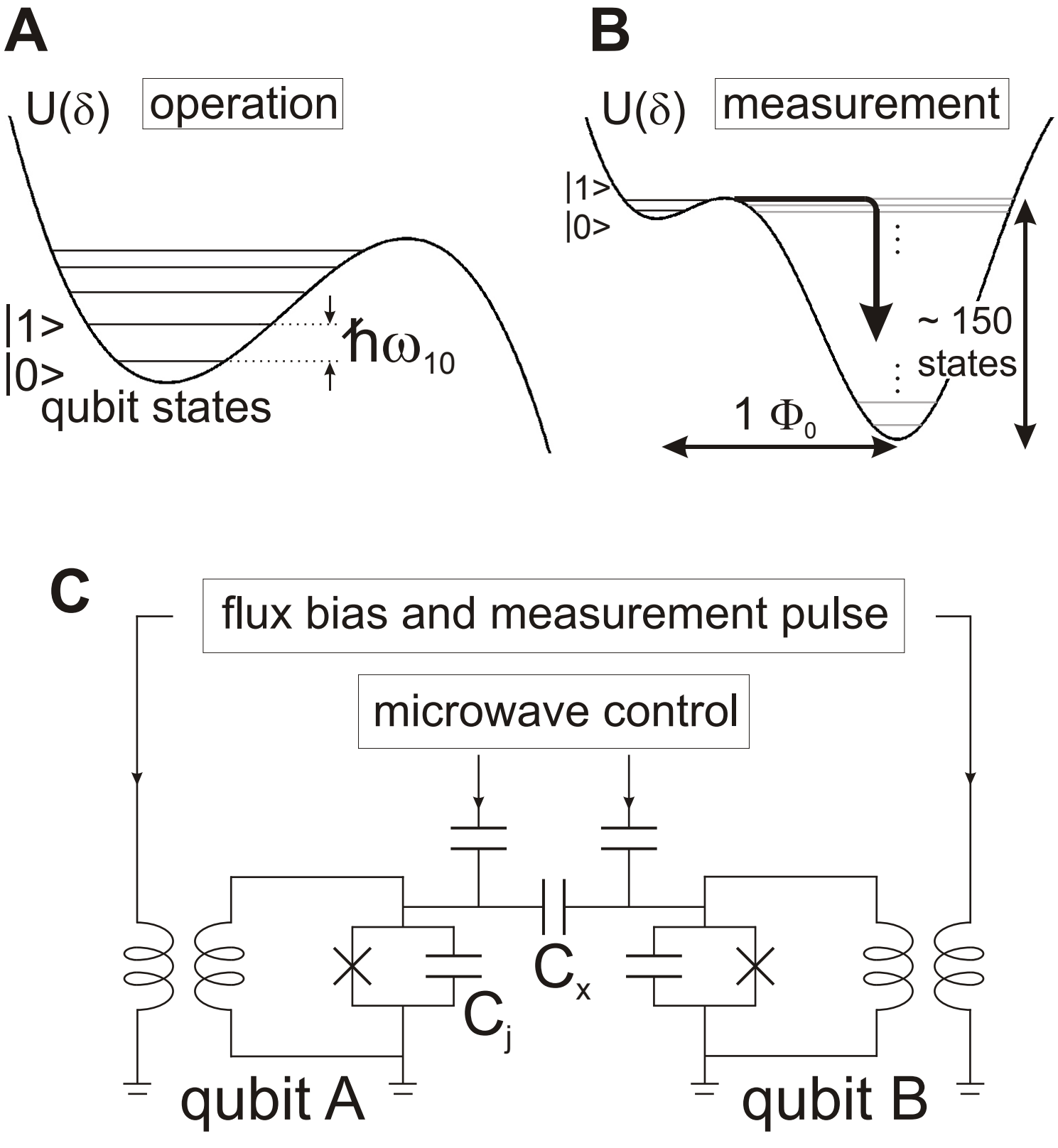
A
U(δ)
operation
|1>
|0>
qubit states
ħω10
B
U(δ)
measurement
|1>
|0>
~ 150
states
1 Φ0
C
flux bias and measurement pulse
microwave control
Cx
Cj
qubit A
qubit B

Fig. 2

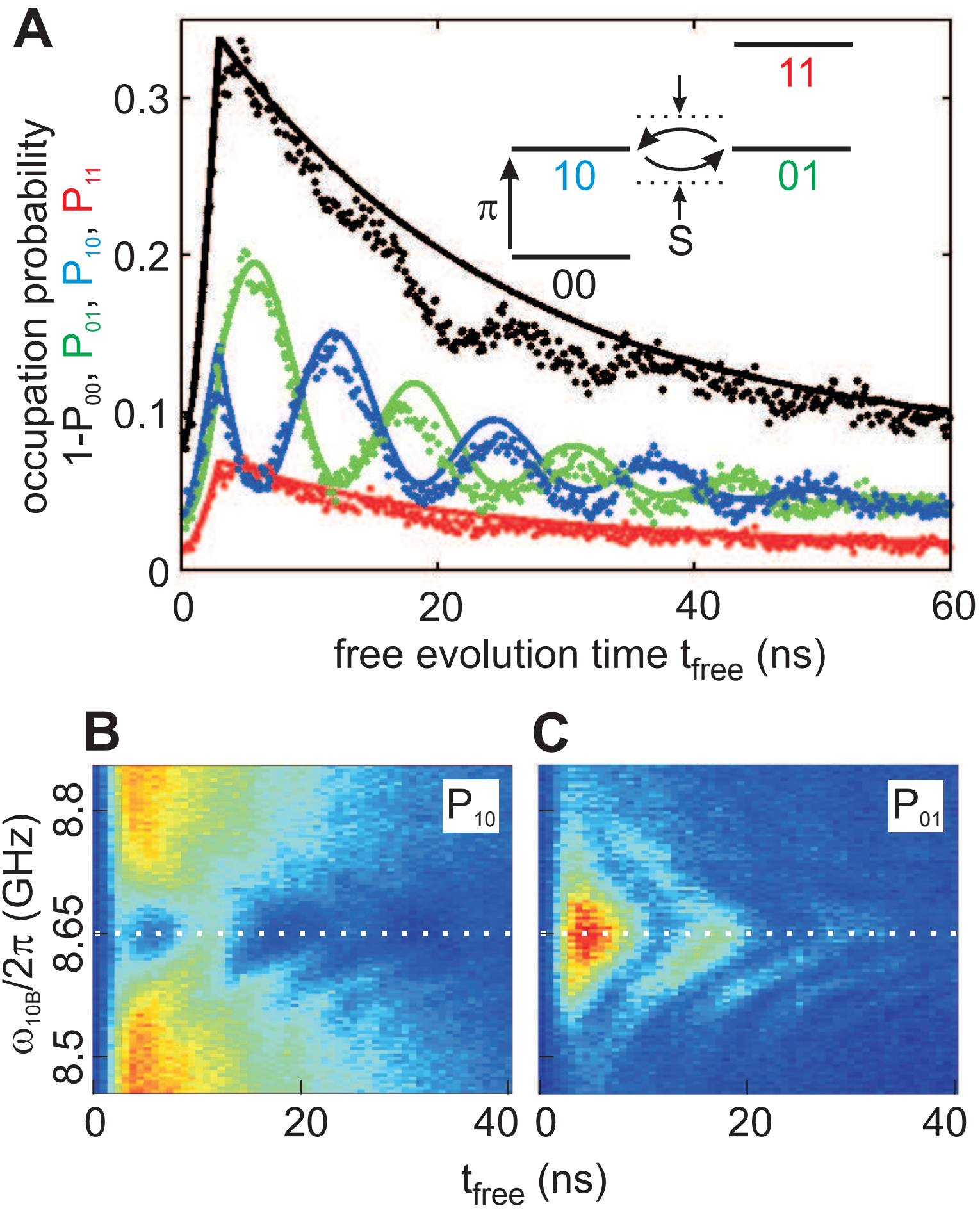
A
occupation probability
1-P00, P01, P10, P11
0.3
0.2
0.1
0
0
20
40
60
free evolution time tfree (ns)
11
10
01
00
π
S
B
C
P10
P01
ω10B/2π (GHz)
8.8
8.65
8.5
0
20
40
tfree (ns)

Fig. 3

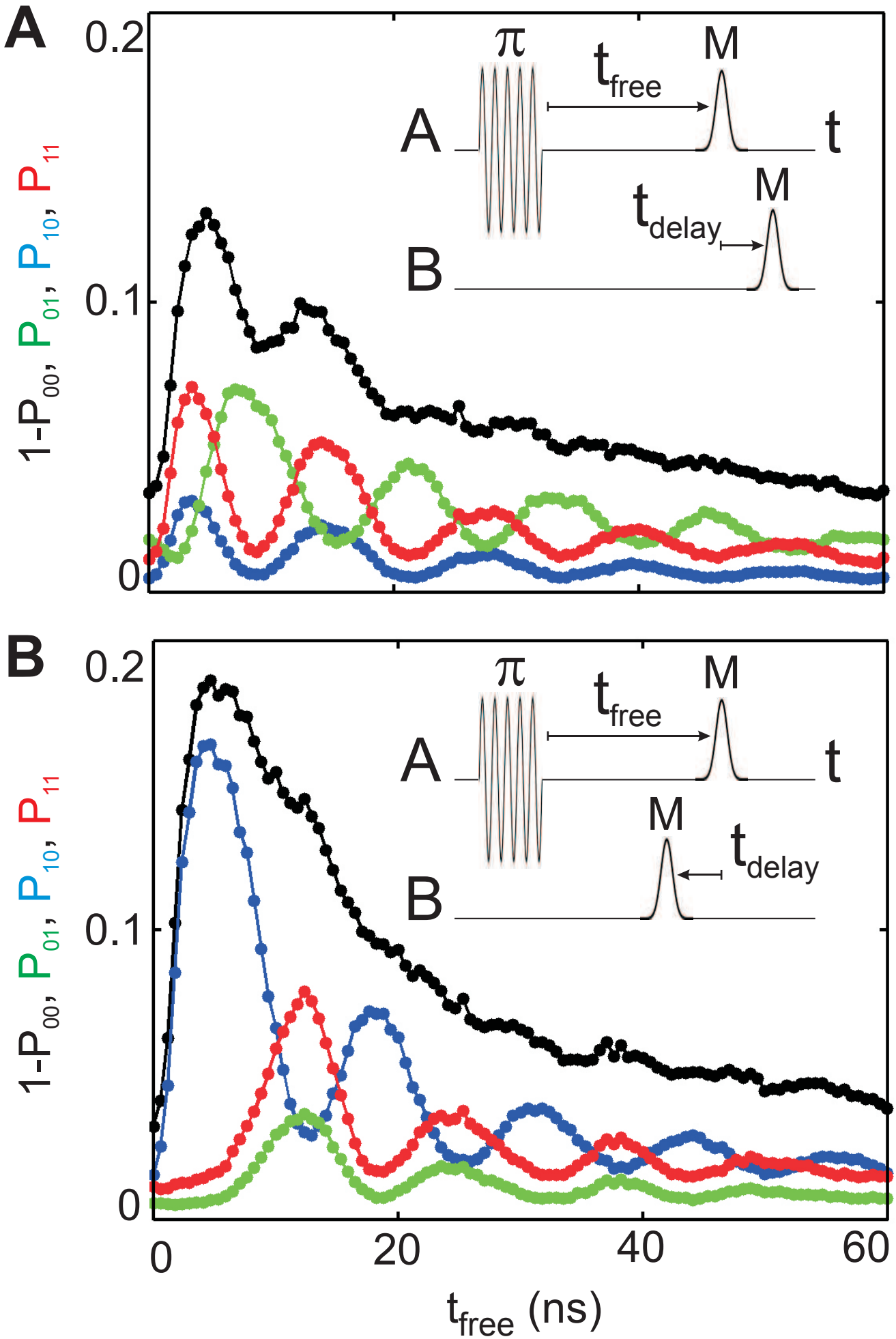

Fig. 4

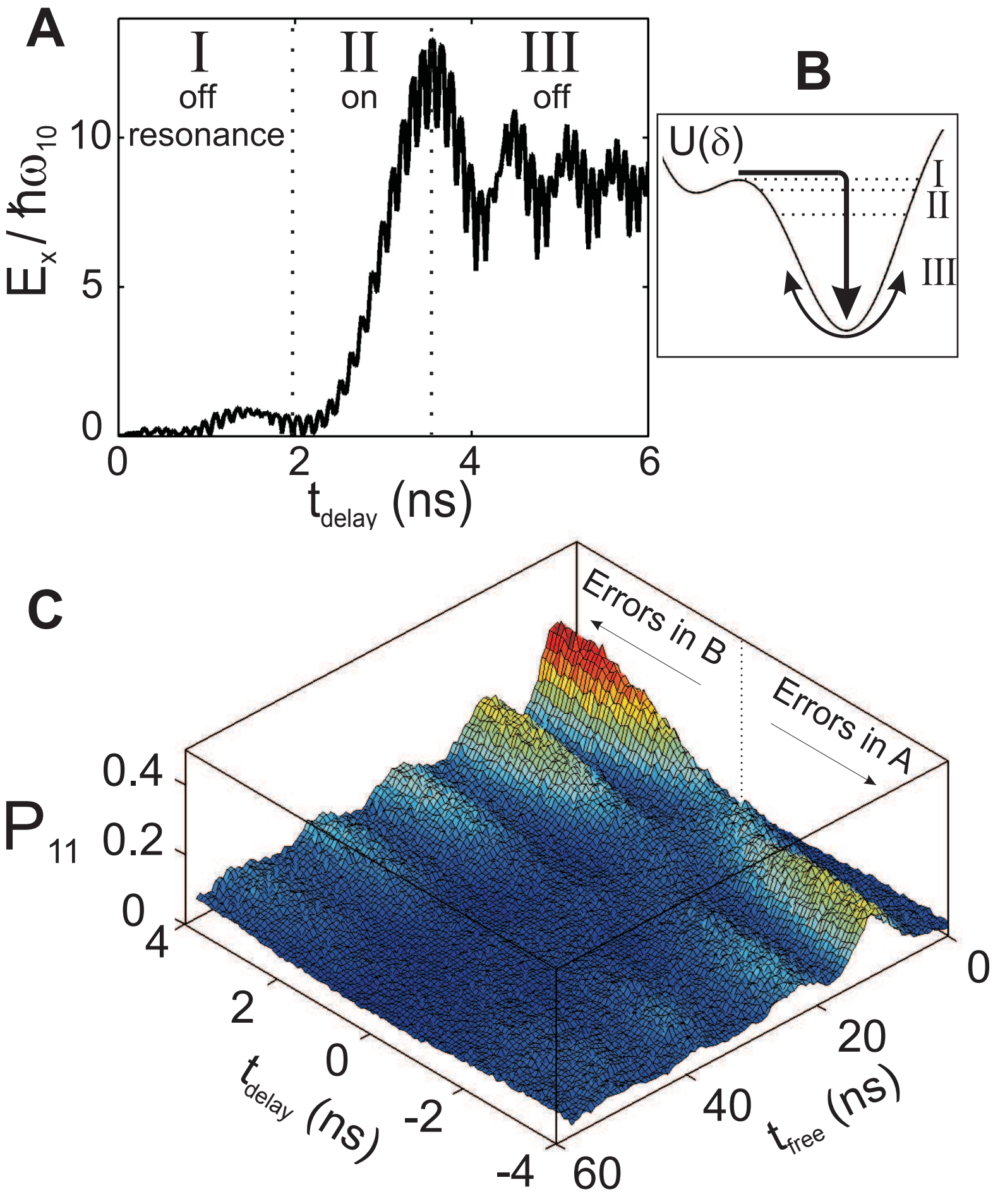
A
I
off
resonance
II
on
III
off
$E_x / \hbar\omega_{10}$
0
5
10
0
2
4
6
t_{delay} (ns)
B
U(δ)
I
II
III
C
Errors in B
Errors in A
P_{11}
0.4
0.2
0
4
2
0
-2
-4
t_{delay} (ns)
0
20
40
60
t_{free} (ns)